Proceedings of the 4th World Congress on Momentum, Heat and Mass Transfer (MHMT'19)
Rome, Italy – April, 2019
Paper No. ICMFHT 130
DOI: 10.11159/icmfht19.130

Modeling of an Air-Assisted Spray Breakup of Urea-Water Solution for SCR Applications

Amit Naik[1,2], Markus Höltermann[1], Eric Lauer[2], Stefan Blodig[2], Friedrich Dinkelacker[1]
[1]Institute for Technical Combustion (ITV), Leibniz University Hannover
Welfengarten 1A, Hannover-30167, Germany
amit.naik@man-es.com
[2]MAN Energy Solutions SE
Stadtbachstr. 1, Augsburg-86153, Germany

Abstract **-** In a selective catalytic reduction (SCR) system for large engines, a quicker evaporation of the urea-water solution (UWS) spray can be achieved through injection with air-assistance. It makes the SCR system more compact, which saves space required for its installation and the cost of manufacturing. A validated CFD study for the air-assisted spray breakup of UWS is not available in the existing literature. In the current work, the Lagrangian-particle-tracking (LPT) model along with the blob approach is used to develop a 3D-CFD simulation method, which can predict the air-assisted spray breakup of UWS in SCR systems. The method can predict sauter mean diameter (SMD), arithmetic mean diameter (AMD) and velocity of droplets. Simulations results are in good agreement with phase Doppler anemometry (PDA) measurements carried out at a hot gas test-rig. The method can also predict the influence of operating conditions on the spray characteristics and helps to determine an optimum mass flow rate of compressed air for the spray breakup process in order to get a desired spray angle and droplets sizes. The aim of the study is to develop a 3D-CFD simulation method for prediction of the air-assisted spray breakup of UWS for SCR applications.

Keywords**:** SCR, AdBlue, urea-water-solution, air-assisted injection, spray breakup, Lagrangian-particle-tracking, Blob method.

1. Introduction

Large diesel engines are widely used for power generation in marine industries. The emissions from diesel engines are toxic and harmful for the environment. Therefore, the stringent emission control standards are necessary. In 2016, the emission control standards for marine diesel engines are revised by International Maritime Organization (IMO) [1]. The selective catalytic reduction (SCR) of nitrogen oxides (NOx) from the exhaust gas of a diesel engine by spraying UWS is considered as one of the most efficient methods. It can reduce 70-90% of NOx from the exhaust gas [2]. It is observed that the air-assisted spray breakup of UWS results into fine droplets, which can evaporate quickly. Quicker evaporation of UWS makes the SCR system compact. These compact SCR systems suit marine applications, where space is always a big concern. Many experimental and CFD investigations are carried out to investigate the spray break up of UWS as well as the diesel injection. Reitz and Bracco [3] have defined the spray breakup regimes for a round liquid jet spray. Some authors have investigated the air-assisted spray breakup experimentally. For example, Marmottant and Villermaux [4] have depicted and analyzed experimentally the successive steps of atomization of a liquid jet when fast gas blows parallel to its surface. C. Dumouchel [5] experimentally investigated the primary breakup of cylindrical liquid jets, flat liquid sheets, air-assisted cylindrical liquid jets and air-assisted flat liquid sheets.

Some researchers also carried out CFD investigations of a spray breakup process without air-assistance. For example, H. Grosshans et al. [6] developed a statistical coupling approach to couple VOF and LPT method to simulate the spray breakup. Tomar et al. [7] performed a multi-scale simulation of the primary atomization using a VOF method coupled with a LPT method. W. Eddelbauer et al. [8] investigated a low-pressure three holes AdBlue injector, which induces swirl while injecting UWS. The authors used a VOF method followed by an externally coupled LPT method to study the spray breakup. R. Reitz [9] investigated atomization and vaporization of a liquid jet injected from a round hole in a compressed gas. The author injected blobs of a liquid that have size equal to the nozzle exit diameter. In another research, J. Beale and R. Reitz [10] modeled a spray atomization using the Kelvin-Helmholtz and Rayleigh-Taylor (KHRT) hybrid model. The authors used

the blob injection model to define the initial size of a droplet. R. Reitz and R. Diwakar [11] calculated the interaction between spray droplets and gas motion close to the nozzle in dense high-pressure sprays. The authors prescribed the atomization by injecting blobs that have a size equal to the nozzle exit diameter.

In the current study, the LPT method combined with the blob approach is used to simulate the air-assisted spray breakup of UWS. Blobs of UWS droplets that have diameter equal to the diameter of the nozzle orifice (for injection of UWS) are injected in a simulation domain. These blobs break in child droplets as per the KHRT breakup model. Later they evaporate/decompose in a surrounding hot exhaust gas. The forces acting on the droplets are taken into account in the LPT modeling. The droplets are captured in an evaluation region and their sauter mean diameters (SMD), arithmetic mean diameter (AMD), and velocities are evaluated. The simulations results are validated with the experiments carried out at the Institute for Technical combustion (ITV), Leibniz University Hannover. The computational resources and time required for these simulations are much lesser than comparable VOF simulations. Also, the results are in good agreement with the experimental measurements. Therefore, this approach can be a good alternative for the VOF method to simulate air-assisted spray breakup of UWS in SCR systems.

The paper is organized in the following manner. The second section discusses the governing equations for the LPT and KHRT model. The third section describes the experimental setup. The fourth section describes simulation methodology, geometry, mesh, operating points and simulations parameters. The fifth section discusses the results and the final section concludes the work.

2. Governing Equations

This section describes the formulation of the Lagrangian particle tracking (LPT) model, which is implemented in the simulation software StarCCM+ [12] by CD-Adapco. Section 2.1 describes the equations of motion for Lagrangian particles followed by Section 2.2, which describes the particles breakup model.

2.1. Particle Equations of Motion

The conservation of momentum for a particle is given by Eq. (1)

$$m_p \frac{d\boldsymbol{v_p}}{dt} = \mathbf{F}_\mathrm{d} + \mathbf{F}_\mathrm{pr} + \mathbf{F}_\mathrm{g} \tag{1}$$

where m_p is the mass of a particle, $\boldsymbol{v}_p$ is the instantaneous particle velocity, $\boldsymbol{F}_d$ is the drag force, $\boldsymbol{F}_{pr}$ is the pressure gradient force, and $\boldsymbol{F}_g$ is the gravity force. Other forces such as Brownian motion, thermophoretic force, and History force are not considered because of their negligible influence on particles motion and breakup [13]. The drag force $\boldsymbol{F}_d$ is calculated by Eq. (2) and the slip velocity $\boldsymbol{v}_s$ is calculated by Eq. (3)

$$\mathbf{F}_\mathrm{d} = \frac{1}{2} C_d \rho A_p |\boldsymbol{v}_s| \boldsymbol{v}_s \tag{2}$$

$$\boldsymbol{v}_s = \boldsymbol{v} - \boldsymbol{v}_p \tag{3}$$

where ρ is the density of a continuous phase, A_p is the projected area of a particle, $\boldsymbol{v}$ is the velocity of the continuous phase, and $\boldsymbol{v_p}$ is the velocity of a particle. C_d is the Schiller-Neumann drag co-efficient [14] of a particle. It is calculate by Eq. (4)

$$C_d = \begin{cases} \frac{24}{Re_p}\left(1 + 0.15 {Re_p}^{0.687}\right) if\ Re_p \leq 10^3 \\ 0.44 \qquad\qquad\qquad\qquad if\ Re_p \geq 10^3 \end{cases} \tag{4}$$

where Re_p is the particle's Reynolds number. The pressure gradient force $\boldsymbol{F}_p$ is calculated by Eq. (5)

$$\mathbf{F}_{\mathrm{p}} = -\boldsymbol{V}_{\boldsymbol{p}}\boldsymbol{\nabla p}_{\boldsymbol{static}} \tag{5}$$

where $\boldsymbol{V}_{\boldsymbol{p}}$ is the volume of a particle and $\boldsymbol{\nabla p}_{\boldsymbol{static}}$ is the gradient of the static pressure in a continuous phase. The gravity force $\boldsymbol{F}_g$ is calculated by Eq. (6)

$$\mathbf{F}_{\mathrm{g}} = m_p\boldsymbol{g} \tag{6}$$

where $\boldsymbol{g}$ is the gravitational acceleration.

2.2. KHRT Breakup Model

The air-assisted spray breakup process of droplets is a result of the forces acting on them due to their acceleration and their slip velocity. These forces can be taken care by the KHRT breakup model [9, 15], which is a combination of two sub models, i.e. Kelvin-Helmholtz (KH) and Rayleigh-Taylor (RT). These models are based on the growth of instabilities on a droplet, and provide expression for their wavelength and frequency. The models are explained below.

2.2.1. Kelvin-Helmholtz (KH) Instabilities

The KH instabilities are due to slip velocity of the droplets. The slip velocity shears small child droplets off a parent droplet as per stripping regime [15]. The time scale τ_{KH} for instabilities is calculated by Eq. (7)

$$\tau_{KH} = \frac{1.894B_1D_P}{\Lambda_{KH}\Omega_{KH}} \tag{7}$$

where B_1 is the breakup time constant. It takes a default value of 10. D_P is the particle diameter and Λ_{KH} is the wavelength of a instability. The size of a child droplet D_{KH} is calculated by Eq. (8)

$$D_{KH} = 2B_0\Lambda_{KH} \tag{8}$$

where B_0 is the model constant. It takes a default value of 0.61.

2.2.2. Rayleigh-Taylor Instabilities

RT instabilities are due to acceleration of the droplets in a continuous phase [16]. They tend to shatter the droplets completely as per catastrophic regime. The time scale τ_{RT} for instabilities is calculated by Eq. (9)

$$\tau_{RT} = \frac{C_\tau}{\Omega_{RT}} \tag{9}$$

where C_τ is the RT time constant, which takes default value of 1. Ω_{RT} is the maximum growth rate. The size of a child droplet D_{RT} is calculated by Eq. (10)

$$D_{RT} = C_3\Lambda_{RT} \tag{10}$$

where Λ_{RT} is the wavelength of RT instabilities and C_3 is the RT time constant, which takes default value of 0.1. The KH and RT models compete with each other. Both the instabilities can grow simultaneously. For smaller times the KH breakup tends to be more dominant, and for longer times the RT breakup.

3. Experimental Setup

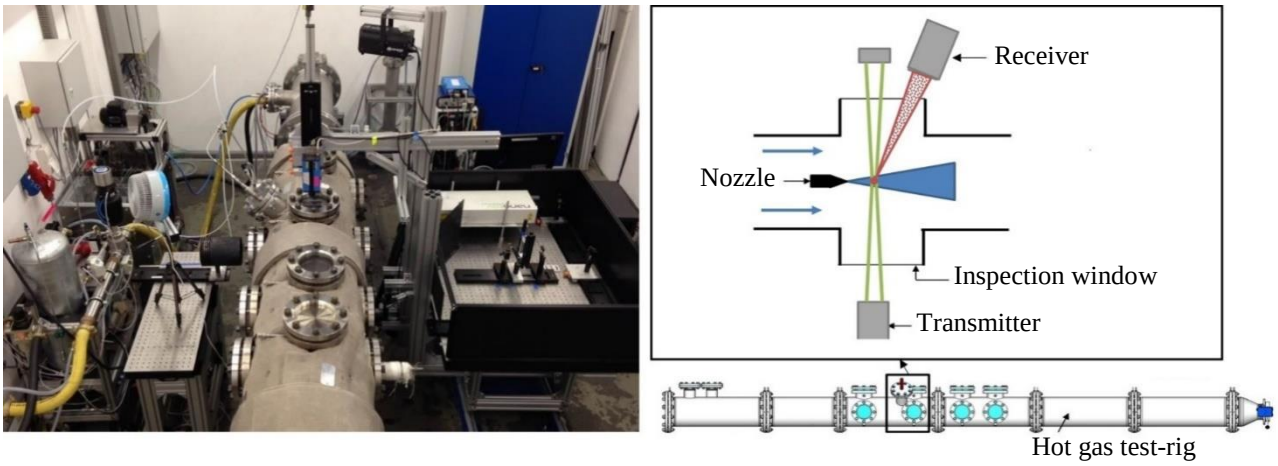

Fig. 1: Hot Gas Test Rig set up for PDA measurements.

To investigate the air-assisted spray breakup of UWS, a hot-gas test-rig, as shown in

Fig. 1, is built at Institute for Technical Combustion (ITV), Leibniz university of Hannover. It has an internal diameter of 300 mm and can be pressured up to 10 bars. The tests are carried out for different operating points i.e. different mass flow rate, pressure, and temperature. The test-rig has inspection windows to carry out optical measurements. The phase Doppler anemometry (PDA), as shown in

Fig. 1, is used to capture the AMD, SMD, and velocity of the UWS droplets. The measurements are carried out at nine points, which are 25 mm away from the nozzle orifice and 5 mm away from each other in radial direction.

4. Numerical Simulation

4.1. Simulation Methodology

The air-assisted spray breakup process is dominated by the compressed air. The internal structure of the nozzle provides swirl to it. Therefore, in order to get the correct velocity profile, it is very important to simulate the flow inside the nozzle. The simulations are carried out in two steps. In the first step, the domain flow including nozzle is simulated until the quasi-steady state is achieved. Then, in the second step, blobs of UWS are injected. When these blobs interact with compressed air, the breakup process begins and child droplets are produced. Because of a swirl in the compressed air, the droplets produced from the breakup process get spread and produce a spray cone. In this way, no predefined spray cone angle is required as a boundary condition. The spray cone angle gets defined by the velocity profile of a compressed air itself. Therefore, in SCR systems, it helps to predict the mixing of NH3 generated from the droplets evaporation in better way than the simulations in which the spray angle is defined as a boundary condition.

The particles count, AMD and velocity of the captured droplets are recorded for every time step in a predefined droplets capturing region and then exported in a tabulated form. The recorded data is used to calculate the SMD.

4.2. Geometry and Mesh

The simulation setup imitates the experiments carried out at a hot gas test-rig as shown in

Fig. 1. The length of the test-rig is 5 m and inner diameter of the test-rig is 300 mm. The polyhedral cells are used for meshing. The base size of 10 mm is set for the mesh. The total cell count is approximately 2.5 million. The prism layers are

used to resolve the boundary layer. A velocity inlet is set as a boundary condition for the hot exhaust gas inflow. A mass flow rate boundary condition is set for the compressed air and UWS. A no-slip wall condition is applied to the wall. The two-layer realizable $k - \varepsilon$ turbulence model is used to take the turbulence into account. The droplets evaluation region is set at 25 mm away from the nozzle orifice.

The air-assisted injector is a two-phase nozzle as shown in Fig. 2**.** The blobs of UWS are injected from the point injector that have diameter equal to the diameter of the nozzle orifice d = 0.5 mm. The compressed air is injected through an orifice that have inner diameter di = 3 mm and outer diameter do = 5 mm, surrounding the orifice for the injection of UWS.

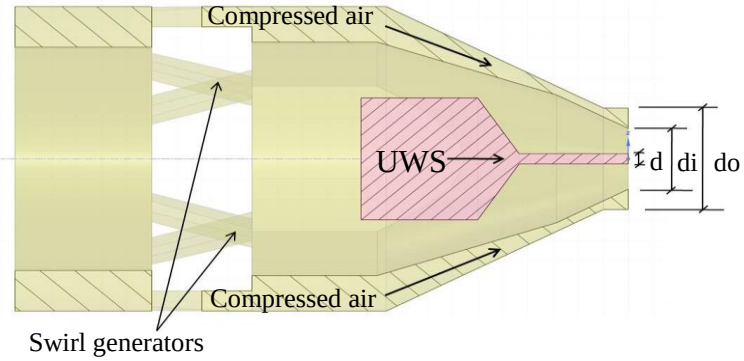

Fig. 2: Two-phase nozzle.

4.3. Operating Points and Simulation Parameters

In order to investigate the spray breakup process, four operating points (OP 1-4) are chosen for simulations. They are tabulated in Table 1, where $P_{exhaust\ gas}$ is the pressure of exhaust gas, $\dot{m}_{UWS}$ is the mass flow rate of UWS, $\dot{m}_{compressed\ air}$ is the mass flow rate of compressed air and d_{blob} is the diameter of a blob of UWS.

Table 1: Operating points.

	OP1	**OP2**	**OP3**	**OP4**
$\boldsymbol{P_{exhaust\ gas}}$ **(bar)**	1	2	2	3
$\boldsymbol{\dot{m}_{UWS}}$ **(kg/hr)**	3	3	3	3
$\boldsymbol{\dot{m}_{compressedair}}$ **(kg/hr)**	8.15	8.15	16.3	16.3
$\boldsymbol{d_{blob}}$**(mm)**	0.5	0.5	0.5	0.5
$\boldsymbol{T_{exhaust\ gas}}$**(°C)**	350	350	350	350

The simulations parameters are tabulated in Table 2.

Table 2: Simulation Parameter.

Parameters	**Values**
Convection scheme	Second order
Temporal discretization	First order
Time-step (sec)	5e-4

5. Results and Discussion

This section compares the simulation and experimental results. It also describes the influence of operating conditions on the spray properties.

5.1. Comparison of Simulations Results with PDA Measurements

The comparison of the simulation results with experiments for OP 1-4 are shown in Fig. 3. The plots compare sauter mean diameters (SMD), also known as D32, arithmetic mean diameters (AMD) and the velocities of the droplets in radial position.

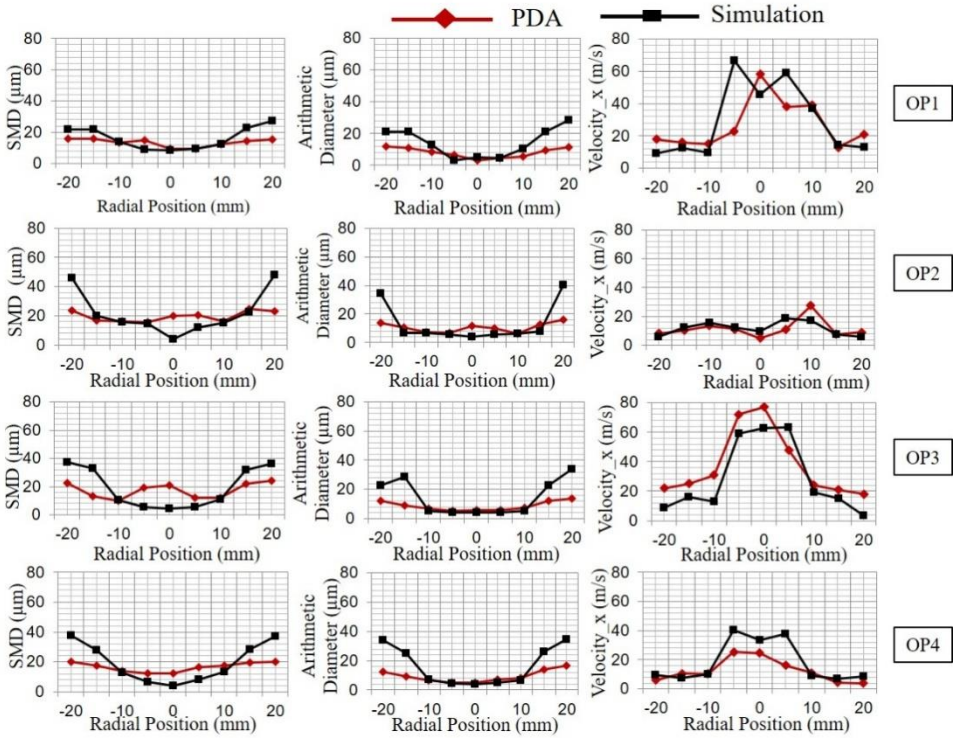

Fig. 3: Comparison of simulations with PDA measurements.

The SMD, AMD and velocity of the droplets for all operating points are in good agreement with the measurements. For all operating points, the trend of the velocity profile of droplets in simulations is very similar to the measurements. As expected, measurements for OP 1-4 show that as the pressure of the exhaust gas increases, the velocity of droplets decreases, which results into slightly larger AMD and SMD. The simulations have succesfully captured this phenomenon.

The velocity of the droplets increases from outer to inner region, which is because the spray is very dense at the center and has many small droplets than the outer region. These droplets have higher velocity than the larger droplets , therefore, the average velocity of the droplets at the core region is higher than the velocity of the droplets at the outer region.

The measurements show that the SMD and AMD are smaller at the center than the outer regions, which is also observed in simulations. The SMD and AMD in simulations at the center region differes slightly from the measurements. This could be due to noise in PDA measurements while capturing very small size droplets where the spray is very dense. In OP2, OP3 and OP4 small droplets along with relatively larger droplets are produced. The PDA measurements has limitations to measure droplets which are smaller than a certain size as it can not differentiate between noise and extremely small droplets. Because of this, many small droplets do not get measured while carrying out PDA measurements. Therefore, the SMD and AMD are over estimated in measurements. On the other hand, in simulations, very small droplets are also captured, which results into smaller SMD and AMD.

5.2. Influence of Operating Conditions on Spray Breakup and Droplets Trajectories

The mass flow rate of a compressed air is one of the factors that influence the trajectories of the droplets and hence, the distribution of NH3 generated from evaporation/decomposition of UWS. Fig. 4 shows that for OP3, where the mass flow rate of compressed air is double than in OP2, the spray-angle is smaller. Therefore, the droplets produced from the breakup process remain confined at the center. They are relatively finer and evaporate faster. Therefore, NH3 generated from the evaporation of droplets also remains confined at the center. Its mixing with the exhaust gas then depends on the turbulence of the surrounding exhaust gas flow. Therefore, even though the increased mass flow of compressed air can produce finer spray, an excessive amount can negatively affect the mixing of NH3 with an exhaust gas. Since NH3 remains confined at the center, NOx at the outer region will not get reduced. Therefore, it will ultimately reduce the performance of the SCR system. Also at the center, where the ammonia for reduction of NOx is more than required, it can cause increased ammonia slip. Therefore, in order to increase the performance of the SCR system, the optimum mass flow rate of compressed air is necessary or the turbulence in the surrounding exhaust gas needs to be higher.

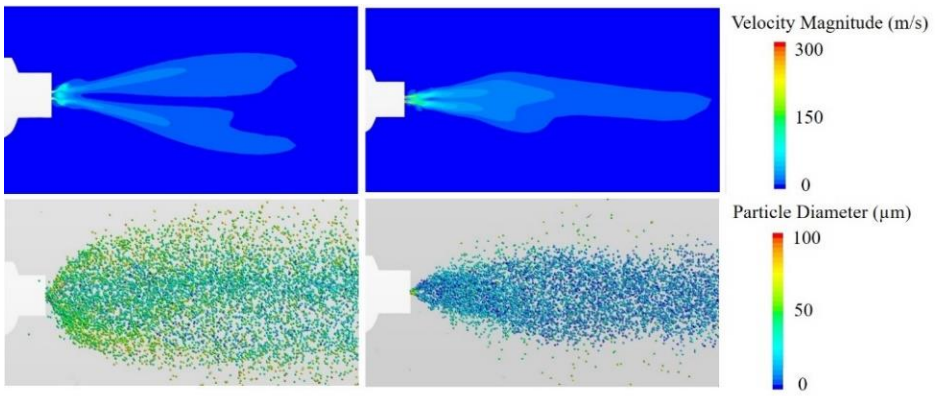

Fig. 4: Influence of the mass flow rate of compressed air on spray trajectories, OP2 (left) and OP3 (right).

The surrounding environment influences the spray breakup process and spray characteristics. Fig. 5 shows the comparison between OP1 (left) and OP2 (right). It shows that the angle of the spread of droplets increases with increased pressure of the surrounding gas. Increase in the pressure of exhaust gas reduces the velocity of the compressed air, which assists the breakup process. The decrease in velocity of the compressed air results into larger size droplets. The large droplets take more time for evaporation; therefore, it increases the risk of deposit formation. In order to minimize this risk, the mass flow rate of compressed air can be increased. The increased mass flow rate of the compressed air can make spray more fine and hence evaporates faster. However, as explained earlier, a large mass flow rate can negatively affect the mixing of NH3 with exhaust gas if the turbulence in exhaust gas is not enough for proper mixing. In such cases, it is necessary to calculate an optimum mass flow rate of the compressed air, which is possible with the method explained in this work.

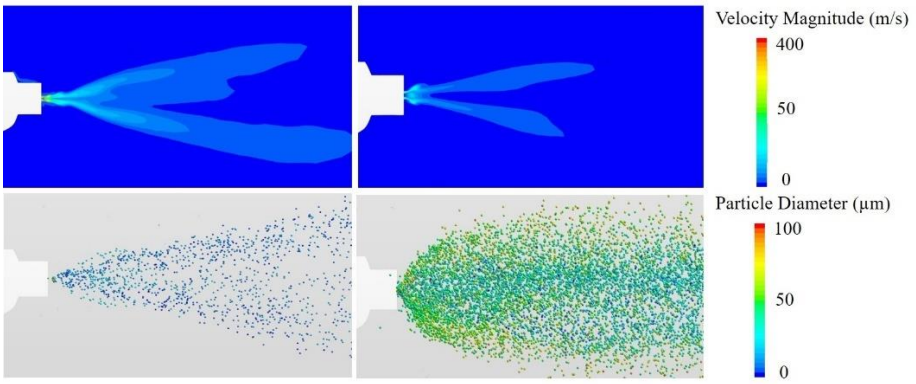

Fig. 5: Influence of the surrounding gas pressure on spray, OP1 (left) and OP2 (right).

6. Conclusion

A 3D-CFD simulation method using the LPT model combined with a blob approach is developed to investigate the air-assisted spray breakup of the urea-water solution in SCR systems. The simulation results show that the spray characteristics such as SMD, AMD and velocity of droplets are in good agreement with measurements carried out at a hot gas test-rig.

The simulation method explained in this work can be used to investigate the influence of operating conditions on spray characteristics. An optimum mass flow rate of the compressed air can be determined to get a desired spray angle and droplets sizes. Therefore, this method can be used to maximize the performance of a SCR system.

An alternative approach to investigate the air-assisted spray breakup process is based on the volume-of-fluid method. However, it requires great amount of computational resources and computational time. The computational resources and time required for the current method to carry out simulations are very less as compared to VOF; therefore, this method could be more feasible for industrial applications.

References

[1] International Maritime Organization, [Online]. Available: http://www.imo.org/en/ourwork/environment/pollutionprevention/airpollution/pages/nitrogen-oxides-(nox)-%E2%80%93-regulation-13.aspx

[2] Air pollution control technology fact sheet, Environmental protection agency, United States, EPA-452/F-03-032 [Online]. Available: https://www3.epa.gov/ttncatc1/dir1/fscr.pdf

[3] R. Reitz and F. Bracco, "Mechanism of breakup of round liquid jets," *Encycl Fluid Mech.*, vol. 3, pp. 233–249, 1986.

[4] P. Marmottant and E. Villermaux, "On spray formation," *J. Fluid Mech*. vol. 498, pp. 73–111, 2004.

[5] C. Dumouchel, "On the experimental investigation on primary atomization of liquid streams," *Exp. Fluids*, vol. 45, pp. 371–422, 2008.

[6] H. Grosshans, Szasz, and L. Fuchs, "Development of an efficient statistical volumes of fluid-Lagrangian particle tracking coupling method," *Int. J. Numer. Meth. Fluids*, vol. 74, pp. 898–918, 2014.

[7] G. Tomar, D. Fuster, S. Zaleski, and S. Popinet, "Multiscale simulations of primary atomization," *Computer and Fluids* vol. 39, pp. 1864–1874, 2010.

[8] W. Edelbauer, F. Birkhold, T. Rankel, Z. Pavlovic, and P. Kolar, "Simulation of the liquid break-up at an AdBlue injector with the volume-of-fluid method followed by off-line coupled Lagrangian particle tracking", ELSEVIER, *Computer and Fluids*, vol. 157, pp. 294–311, 2017.

[9] R. D. Reitz, "Modeling Atomization Processes in High-Pressure Vaporizing Sprays", *Atomization and Spray Technology*, vol. 3, pp. 309–337, 1987.

[10] J. Beale and R. Reitz, "Modeling spray atomization with the Kelvin-Helmholtz/Rayleigh-Taylor hybrid model", *Atomization and Sprays*, vol. 9, issue 6, pp. 623-650, 1999.

[11] R. D. Reitz, and R. Diwakar, "Structure of High-Pressure Fuel Sprays", SAE Paper 870598, 1987.

[12] Starccm+ documentation, [Online]. Available: https://mdx.plm.automation.siemens.com/star-ccm-plus
[13] H. Ström, A. Lundström, and B. Andersson, “Choice of urea-spray models in CFD simulations of urea-SCR systems“, *Chemical engineering journal*, vol. 150, pp. 69-82, 2009.
[14] L. Schiller and A. Naumann. “Über die grundlegenden Berechnungen bei der Schwerkraftaufbereitung”, *VDI Zeits.*, vol. 77, no. 12, pp. 318–320, 1933.
[15] M. Patterson and R. Reitz, “Modeling the Effects of Fuel Spray Characteristics on Diesel Engine Combustion and Emission”, SAE Paper 980131, 1998.